Density functional theory for freezing transition of vortex-line liquid with periodic layer pinning

Xiao Hu*, Mengbo Luo*,†, and Yuqiang Ma*,‡

*Computational Materials Science Center, National Institute for Materials Science, Tsukuba 305-0047, Japan
†Department of Physics, Zhejiang University, Hangzhou 310027, People's Republic of China
‡Department of Physics, Nanjing University, Nanjing 210093, People's Republic of China
(Dated: February 2, 2008)

By the density functional theory for crystallization, it is shown that for vortex lines in an underlying layered structure a smectic phase with period $m = 2$ can be stabilized by strong layer pinning. The freezing of vortex liquid is then two-step, a second-order liquid-smectic transition and a first-order smectic-lattice transition. DFT also indicates that a direct, first-order liquid-lattice transition preempts the smectic order with $m \geq 3$ irrespectively of the pinning strength. Possible $H - T$ phase diagrams are mapped out. Implications of the DFT results to the interlayer Josephson vortex system in high-T_c cuprates are given.

PACS numbers: 74.25.Dw, 74.25.Qt

It is now well established that the Abrikosov vortex lattice in type II superconductors [1] melts via a thermodynamic first-order transition [2]. However, much less consensus has been reached on the possible phases and melting process of interlayer Josephson vortex lattice where layer pinning is essential. A Lorentz-force independent dissipation was found in $Bi_2Sr_2CaCu_2O_{8+y}$ at $H = 5T$ parallel to the ab-plane [3], which is possibly a signature of a Kostlitz-Thouless (KT) phase [4, 5, 6]. On the other hand, transport experiments conducted in $YBa_2Cu_3O_{7-\delta}$ suggested a second-order softening of the vortex lattice [7], which can be accounted for by a smectic phase [8]. A recent computer simulation found continuous meltings and a KT-type intermediate phase above a multicritical field [9, 10].

As a general theory for crystallization, the density functional approach was formulated by Ramakrishnan and Yussouff [11] (See also [12]). The basic idea of the density functional theory (DFT) is to describe the lattice phase and the freezing transition by the direct pair correlation function (DPCF) in liquid phase, which in turn can be evaluated from macroscopic quantities such as the average density and temperature. At the clean limit, both the first-order nature of the vortex-line liquid freezing and quantitative aspects such as the Lindemann number have been successfully captured by DFT [13]. Later on, DFT was used to investigate vortex-line systems with point-like [14] and columnar [15] pinning centers.

In the present work, we apply DFT to explore the freezing of vortex-line liquid subject to periodic layer pinning [16, 17]. As it is hard to evaluate the DPCF with finite interlayer Josephson coupling [13], which is essential in the present case, we will not try to draw the detailed phase diagram. Instead, we adopt the DPCF and the layer pinning strength as parameters to explore the possible freezing processes. This approach turns out to be fruitful: A vortex smectic phase with more vortex lines in every other layers (period $m = 2$) is observed at strong layer pinning. When the smecitc phase is present, the freezing of vortex liquid is two-step, a second-order liquid-smectic and a first-order smectic-lattice transition. A direct, first-order liquid-lattice transition preempts the smectic order with $m \geq 3$ irrespectively of the pinning strength. Possible topologies of $H - T$ phase diagrams are figured out.

The free energy of a vortex-line system measured from the uniform liquid is given by [12, 13, 18]

$$\beta \Delta \mathcal{F} = \int d^2r \sum_n \left[\rho_n(\mathbf{r}) \ln \frac{\rho_n(\mathbf{r})}{\rho_0} + (A-1)\delta\rho_n(\mathbf{r}) \right]$$
$$- \frac{1}{2} \int d^2r d^2r' \sum_{n,n'} \delta\rho_n(\mathbf{r})\delta\rho_{n'}(\mathbf{r}')C(\mathbf{r}-\mathbf{r}', n-n')$$
$$- \int d^2r \sum_n \delta\rho_n(\mathbf{r})\beta V_{\rm p}\cos(qz), \qquad (1)$$

where $\delta\rho(\mathbf{r}) = \rho(\mathbf{r}) - \rho_0$ with ρ_0 the average areal vortex density and $C(\mathbf{r}-\mathbf{r}', n-n')$ the DPCF. The summations are taken over vortex segments along the magnetic field $(B\|\mathbf{y})$, and the integrals over the transverse directions $\mathbf{x}$ and $\mathbf{z}$, with $\mathbf{z}\|c$ axis. $V_{\rm p}$ is the pinning energy per vortex segment.

By means of the variational calculus, the free-energy density per vortex segment of a vortex lattice is found as

$$\frac{\beta \Delta \mathcal{F}}{N_{xz}N_y} = -A + \frac{1}{2}s_{\rm u}\sum_{\mathbf{K}} \rho_{\mathbf{K}}^2 C(\mathbf{K}, 0), \qquad (2)$$

with $s_{\rm u} = 1/\rho_0$ the area of real-space unit cell (u.c.), N_{xz} the number of unit cells and N_y the number of vortex segments, the summation over the reciprocal lattice vectors (RLVs), $\rho(\mathbf{r}) = \rho_0 + \sum_{\mathbf{K}} \rho_{\mathbf{K}}\exp(i\mathbf{K}\cdot\mathbf{r})$, and $C(\mathbf{k}, 0) = \int d^2r \sum_n C(\mathbf{r}, n)\exp(-i\mathbf{k}\cdot\mathbf{r})$. The chemical potential A is given by

$$A = \ln\frac{1}{s_{\rm u}}\int_{\rm u.c.} d^2r e^{\sum_{\mathbf{K}} \rho_{\mathbf{K}} C(\mathbf{K},0)\exp(i\mathbf{K}\cdot\mathbf{r})+\beta V_{\rm p}\cos(qz)}, \quad (3)$$

with the integral over the unit cell. The lattice phase is characterized by the non-vanishing Fourier components of the vortex density, which thus serve as the order parameters for the freezing transition. Following previous studies [12, 13], we adopt a few order parameters in the present work confirming that more will not change the conclusions qualitatively.

Because of the linear coupling with the vortex density, the layer pinning V_p appears only in the chemical potential A in the free-energy density. The layer pinning is effective when the pinning wavenumber q coincides with one of the RLVs. As the DPCF $C(\mathbf{K}, 0)$ decreases quickly as going to higher shells of RLVs, the layer pinning is most important when its wave vector coincides with one of the primitive RLVs.

For weak magnetic fields, vortices reside in a periodic subset of block layers with period ms where s is the layer spacing. For large m, the pinning energy term in Eq.(3) decouples from the lattice-order term and only modifies the measure of the integral of the lattice potential. In such a case the layer pinning is irrelevant to the phase transition. The freezing process is then essentially the same with the Abrikosov lattice with the scaling by the anisotropy parameter [19]. It takes numerics shown below to see to what extension that the large-m limit governs the freezing phenomenon .

Vortex segment and layer pinning energy– When a single vortex line is placed in a periodic layer pinning potential, a kink (kernel) presumes a metastable state in which a part of the vortex line cross the pinning barrier and reside in the neighbor energy valley. The crossing takes place within the length scale $L_\mathrm{wall} \simeq s\sqrt{\gamma\epsilon_0/4U_\mathrm{p}}$, where $\gamma = \lambda_\mathrm{c}/\lambda_\mathrm{ab}$, $\epsilon_0 = (\phi_0/4\pi\lambda_\mathrm{ab})^2$, U_p the pinning energy per unit length [8, 17]. The pinning energy is $V_\mathrm{p} = s\sqrt{\gamma\epsilon_0 U_\mathrm{p}}$, and the kink length defined as the separation between two crossings is $L_\mathrm{kink} = L_\mathrm{wall}\exp(2\beta V_\mathrm{p})$ [8]. The physical choice of the vortex segment in the free-energy functional (1) is therefore the kink with the pinning energy per kink V_p. The above estimates are physically meaningful when L_kink is sufficiently larger than L_wall, or equivalently βV_p is large enough. Numerically, for YBa$_2$Cu$_3$O$_{7-\delta}$ with $T_c = 92K$, $\kappa = 100$, $\gamma = 8$, $\lambda_{ab}(0) = 1000\mathring{A}$ and $s = 12\mathring{A}$, one has $L_\mathrm{wall} \simeq 10s$, $L_\mathrm{kink} \simeq 60s$, and $\beta V_\mathrm{p} \simeq 0.8$ at $T = 88K$. As temperature decreases, βV_p increases linearly to $\beta V_\mathrm{p} \simeq 4.3$ at $T = 80K$, L_wall decreases slowly and L_kink increases exponentially. For Bi$_2$Sr$_2$CaCu$_2$O$_{8+y}$ with $T_c = 90K$, $\kappa = 100$, $\gamma = 150$, $\lambda_{ab}(0) = 2000\mathring{A}$ and $s = 15\mathring{A}$, one has $\beta V_\mathrm{p} \simeq 0.2$ at $T = 84K$, which increases linearly to $\beta V_\mathrm{p} \simeq 0.3$ at $T = 78K$.

Lattice unit cell– The vortex lattice structure in the presence of layer pinning is nontrivial. In an anisotropic material *without* layer modulation, there are two stable directions of triangle vortex lattice, which are described by the following two unit cells [5]: Type A: $\mathbf{a}_1 = C\sqrt{\gamma}\mathbf{x}, \mathbf{a}_2 = \frac{C\sqrt{\gamma}}{2}\mathbf{x} + \frac{C\sqrt{3}}{2\sqrt{\gamma}}\mathbf{z}$; Type B: $\mathbf{a}_1 = \frac{C}{\sqrt{\gamma}}\mathbf{z}, \mathbf{a}_2 = \frac{C\sqrt{3\gamma}}{2}\mathbf{x} + \frac{C}{2\sqrt{\gamma}}\mathbf{z}$, with $C^2 = 2\phi_0/\sqrt{3}B$. The associated
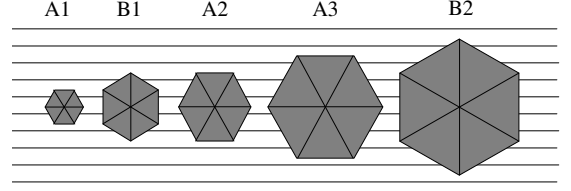

FIG. 1: Real-space unit cells commensurate with layer modulation. The x direction is rescaled with the anisotropy parameter γ. A and B are for the type of unit cell, and the number denotes m defined in text.

RLVs are Type A: $\mathbf{b}_1 = \frac{2\pi}{C\sqrt{\gamma}}\mathbf{x} - \frac{2\pi\sqrt{\gamma}}{C\sqrt{3}}\mathbf{z}, \mathbf{b}_2 = \frac{4\pi\sqrt{\gamma}}{C\sqrt{3}}\mathbf{z}$; Type B: $\mathbf{b}_1 = -\frac{2\pi}{C\sqrt{3\gamma}}\mathbf{x} + \frac{2\pi\sqrt{\gamma}}{C}\mathbf{z}, \mathbf{b}_2 = \frac{4\pi}{C\sqrt{3\gamma}}\mathbf{x}$.

In DFT the reduction of free energy of crystallization is evaluated by the DPCF of liquid, which is isotropic after the space-rescaling with the anisotropy parameter. Just above the freezing, there appears a sharp peak in the DPCF at $k_0 = 4\pi/\sqrt{3}C$ associated with the uniform vortex density of the rescaled, *isotropic* liquid. The reduction of free energy is maximal when the RLVs of a candidate lattice coincide with k_0 in magnitude. It is easy to see that the two lattice structures listed above match this condition.

On the other hand, the vortex lattice is requested to be commensurate with the underlying layer modulation in DFT, which is reasonable for layered superconductors like high-T_c cuprates. This makes the pinning energy equivalent for different lattice structures. Therefore, at the following sequence of the magnetic fields $H_1 = \sqrt{3}\phi_0/2\gamma s^2$, $H_2 = \phi_0/2\sqrt{3}\gamma s^2$, $H_3 = \sqrt{3}\phi_0/8\gamma s^2$, $H_4 = \phi_0/6\sqrt{3}\gamma s^2$, and $H_5 = \phi_0/8\sqrt{3}\gamma s^2$, ..., the vortex lattices depicted in Fig. 1 resume minimal free energy. The stable lattice structure at magnetic fields nearby those listed above should be the same with those in Fig. 1 except for that the vortex separation in the x direction is adjusted in order to accommodate the vortex density. The ground-state lattice structure changes when two freezing DPCFs coincide. The lattice structure with a smaller freezing DPCF is achieved at a higher temperature and is stable for the given magnetic field. Possible first-order transition between different lattices upon sweeping the magnetic field at fixed temperature was addressed in Ref.[20].

Freezing transitions– We now proceed to investigate the freezing process and nature of phase transition when the lattice structure is given and the DPCF is swept. This corresponds to reducing temperature at given magnetic fields. We will focus on the sequence of magnetic fields listed above, where the vortex lattice are *naturally* commensurate with the layer structure. Although analyses on other magnetic fields are *technically* cumbersome as $C(\mathbf{K}, 0)$'s assume different values even on the same shells of RLVs, the possible phases and nature of phase transition should be the same. As read from Eqs. (2) and (3),
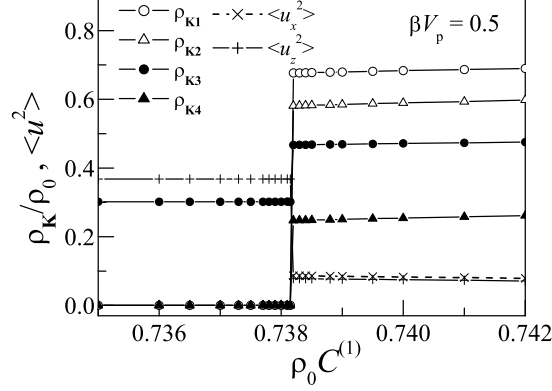
FIG. 2: First-order freezing into the lattice structure A2 for $\beta V_{\mathrm{p}} = 0.5$, with $C^{(3)} = 0.3C^{(1)}$. Thermal fluctuations $\langle u_x^2 \rangle$ and $\langle u_z^2 \rangle$ are normalized by $(\gamma s)^2$ and s^2 respectively. $\langle u_x^2 \rangle = \infty$ for $\rho_0 C^{(1)} < 0.7382$.
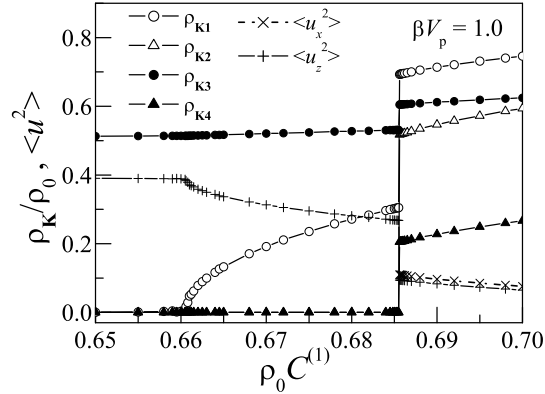

FIG. 4: $\rho_0 C^{(1)} - \beta V_{\mathrm{p}}$ phase diagram for the lattice A2. Inset: mean squared displacements, normalized by $(\gamma s)^2$ and s^2 in the x and z directions respectively, evaluated along the first-order phase boundary.

FIG. 3: Two-step freezing, a second-order and a first-order transitions, into the lattice structure A2 and an intermediate smectic phase for $\beta V_{\mathrm{p}} = 1$, with $C^{(3)} = 0.3C^{(1)}$. Thermal fluctuations $\langle u_x^2 \rangle$ and $\langle u_z^2 \rangle$ are normalized by $(\gamma s)^2$ and s^2 respectively. $\langle u_x^2 \rangle = \infty$ for $\rho_0 C^{(1)} < 0.6856$.

freezing transitions for different anisotropy parameter γ are governed by the same set of $C(\mathbf{K}, 0)$'s as functions of V_{p} and m. This corresponds to the scaling property addressed in Ref.[19], apart from the layer pinning effect.

For A1 in Fig. 1, the present system is equivalent to colloids under laser radiation addressed in Ref.[18]. As the pinning energy increases, the freezing switches from first order to continuous at a tricritical point at $\beta V_{\mathrm{p}} \simeq 0.212$ and $\rho_0 C^{(1)} \simeq 0.748$. The notation with $C^{(i)}$ referring to $C(\mathbf{K}, 0)$ for $\mathbf{K}$ on the i-th shell of RLVs is adopted in the present Letter.

For A2, we use four order parameters $\rho_{\mathbf{K}}$ where $\mathbf{K}1 = \mathbf{b}_2$, $\mathbf{K}2 = \mathbf{b}_1$, $\mathbf{K}3 = 2\mathbf{b}_2$, and $\mathbf{K}4 = 2\mathbf{b}_1$ with $\mathbf{b}_2 = \pi/s z$. A finite $\rho_{\mathbf{K}3}$ characterizes the modulated liquid. The freezing is first order at low pinning energy such as $\beta V_{\mathrm{p}} = 0.5$ depicted in Fig. 2, where all order parameters except for the trivial one set up discontinuously. At large pinning energy, a phase characterized by $\rho_{\mathbf{K}1} > 0$
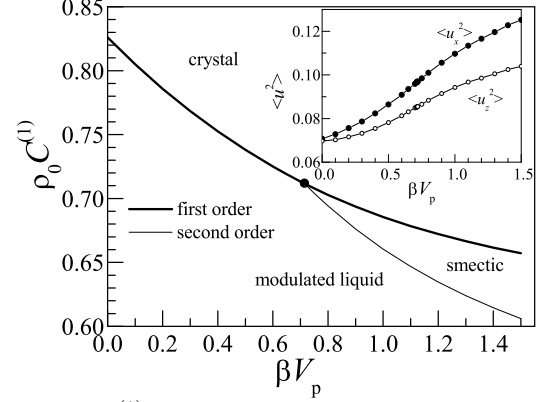
and $\rho_{\mathbf{K}2} = \rho_{\mathbf{K}4} = 0$ appears via a second-order phase transition as shown explicitly in Fig. 3 for $\beta V_{\mathrm{p}} = 1$. The vortex density modulation is associated with a wave number half of the underlying layer structure, corresponding to more vortices in every other layers; the system behaves as liquid in in-plane directions. This is the smectic order addressed in Ref.[8], and the liquid-smectic transition is in the Ising universality class since $m = 2$. As DPCF increases, the full lattice order appears via a first-order transition. The $\rho_0 C^{(1)} - \beta V_{\mathrm{p}}$ phase diagram for A2 is presented in Fig. 4, with a multicritical point at $\rho_0 C^{(1)} \simeq 0.714$ and $\beta V_{\mathrm{p}} \simeq 0.712$. This is one of the central observations of the present DFT study.

Similar analysis has been performed for A-type lattice with $m \geq 3$, using $C^{(2)} = 0.5C^{(1)}$, $C^{(3)} = 0.3C^{(1)}$, $C^{(5)} = 0.1C^{(1)}$ and so on. In contrast with A1 and A2, we cannot find the smectic phase and continuous transition up to huge pinning energy accessible in numerics. This DFT prediction is different from the analysis in Ref.[8].

For unit cell of type B, the crystallization is always one step and first order. In this case no primitive Bragg peak matches with the layer modulation, and thus the layer pinning is much ineffective compared with the lattices A1 and A2. As the result, the six primitive Bragg peaks appear simultaneously which is associated with a first-order transition. The first-order melting transition observed in Monte Carlo simulations for $B = \phi_0/32s^2$ and $\gamma = 8$ [9, 10] is in accordance with the DFT, since the lattice structure is B1. In principle, there might be a smectic phase associated with the two Bragg spots $\mathbf{K} = (0, \pm\pi/s)$ on the second shell of RLVs for B2. However, numerical analysis reveals that this situation is not realized since the layer pinning is at the 6th shell of RLVs and the interaction with those on the 2nd shell is very weak.

Phase diagram – Although the detailed freezing curve cannot be drawn without calculations on DPCF at given magnetic fields and temperatures, we are able to categorize possible $H - T$ phase diagrams based on the above
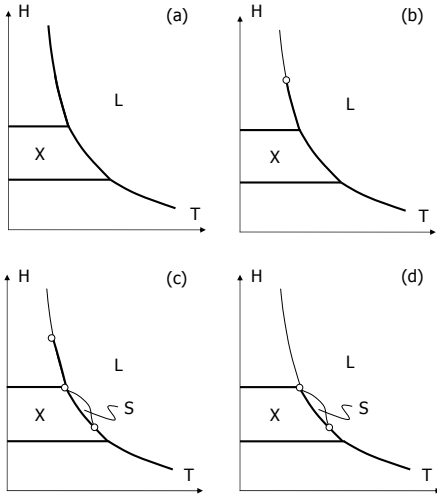
FIG. 5: Possible $H - T$ phase diagrams for vortex lines in periodic layer pinning potential from DFT, with L, X and S abbreviating liquid, lattice and smectic respectively. The thick (thin) curves denote first(second)-order phase boundaries. Multicritical points are marked by open circles. The horizontal phase boundaries are drown only for B1-A2 (A1-A2 in (d)) and A2-A3 transitions.

analyses. Figure 5(a) corresponds to a system of weak layer pinning, in which freezing is always first order. The two horizontal phase boundaries are between lattices structures B1-A2 and A2-A3 [20]. Note that similar phase boundaries may be observed at lower magnetic fields, and that the lattices A1 and B1 can be tuned into each other through crossover. In Fig. 5(b), the freezing transition into vortex lattice A1 is of second order at high magnetic fields where the freezing temperature is low and the layer pinning is strong enough. At even stronger layer pinning, a smectic phase appears and transforms into

lattice A2 upon cooling as shown in Fig. 5(c). As the magnetic field increases to the regime where the lattice B1 presumes the ground state, the smectic phase shrinks to zero. It is possible practically that the lattice B1 is unstable comparing with other lattice structures, resulting in Fig. 5(d). No further complex phase diagram is expected from DFT.

Discussions– Based on the DFT analysis and experimental phase diagrams for $H < 10T$ [7, 21], the $m = 2$ smectic phase is expected for $YBa_2Cu_3O_{7-\delta}$ around $H = H_3 \simeq 39T$. No smectic phase is plausible for $H \leq H_4 = \phi_0/6\sqrt{3}\gamma s^2 \simeq 17T$. Layer pinning may be too weak in $Bi_2Sr_2CaCu_2O_{8+y}$ to stabilize the smectic.

Since DFT only treats the RLVs, it is unable to describe quasi long-range orders. A KT phase is therefore out of the scope where DFT can reach. With this drawback of DFT in mind, one may notice that the tricritical point for A1 lattice in Fig. 5, which should exist in both $YBa_2Cu_3O_{7-\delta}$ and $Bi_2Sr_2CaCu_2O_{8+y}$, corresponds to the multicritical point above which an intermediate KT phase is observed in computer simulations [10].

As displayed in the inset of Fig. 4, thermal fluctuations are more anisotropic than the anisotropy parameter γ, which is clearly caused by the layer pinning. This anisotropy exists irrespectively of the existence of smectic phase, and thus cannot be taken as a precursor of a partial melting [22]. In presence of layer pinning the Lindemann numbers are not constant any more.

One may expect that the results derived above apply to two-dimensional (2D) systems [12] with periodic line pinning. It is noticed however that thermal fluctuations are more important in 2D as addressed in Ref.[23].

[1] A. A. Abrikosov, Zh. Eksp. Teor. Fiz. **32**, 1442 (1957) [Phys. JETP **5**, 1174 (1957)].
[2] G. Blatter *et al.*, Rev. Mod. Phys. **66**, 1125 (1994); G. W. Crabtree, and D. R. Nelson, Phys. Today **45**, 38 (1997); T. Nattermann and S. Scheidl, Adv. Phys. **49**, 607 (2000).
[3] Y. Iye *et al.*, Physica **159C**, 433 (1989).
[4] K. B. Efetov, Sov. Phys. JETP **49**, 905 (1979).
[5] B. I. Ivlev *et al.*, J. Low Temp. Phys. **80**, 187 (1990).
[6] G. Blatter *et al.*, Phys. Rev. Lett. **66**, 2392 (1991).
[7] W. K. Kwok *et al.*, Phys. Rev. Lett. **72**, 1088 (1994).
[8] L. Balents and D. R. Nelson, Phys. Rev. B **52**, 12951 (1995); L. Balents and L. Radzihovsky, Phys. Rev. Lett. **76**, 3416 (1996).
[9] X. Hu and M. Tachiki, Phys. Rev. Lett. **85**, 2577 (2000).
[10] X. Hu and M. Tachiki, cond-mat/0406183.
[11] T. V. Ramakrishnan and M. Yussouff, Phys. Rev. B **19**, 2775 (1979).
[12] T. V. Ramakrishnan, Phys. Rev. Lett. **48**, 541 (1982).
[13] S. Sengupta *et al.*, Phys. Rev. Lett. **67**, 3444 (1991); I. F. Herbut and Z. Tešanović, Phys. Rev. Lett. **73**, 484 (1994); G. I. Menon *et al.*, Phys. Rev. B **54**, 16192 (1996).
[14] G. I. Menon and C. Dasgupta, Phys. Rev. Lett. **73**, 1023 (1994).
[15] C. Dasgupta and O. T. Valls, Phys. Rev. Lett. **87**, 257002 (2001); *ibid*, Phys. Rev. B **66**, 064518 (2002).
[16] M. Tachiki and S. Takahashi, Solid State Commun. **70**, 291 (1989).
[17] A. Barone *et al.*, J. of Super. **3**, 155 (1990).
[18] J. Chakrabarti *et al.*, Phys. Rev. Lett. **73**, 2923 (1994).
[19] G. Blatter *et al.*, Phys. Rev. Lett. **68**, 875 (1992).
[20] L. Bulaevskii and J. R. Clem, Phys. Rev. B **44**, 10234 (1991).
[21] A. Schilling *et al.*, Phys. Rev. B **65**, 054505 (2002).
[22] X. Hu and Q.H. Chen, Phys. Rev. Lett. **92**, 209701 (2004).
[23] E. Frey *et al.*, Phys. Rev. Lett. **83**, 2977 (1999).